Acc. Chem. Res. **1999,** 32, 975−982

Supermolecules by Design

DANA L. CAULDER AND
KENNETH N. RAYMOND*

*Department of Chemistry, University of California,
Berkeley, California 94720-1460*

Received January 25, 1999

High-Symmetry Clusters in Nature

Supramolecular chemistry describes the spontaneous assembly of noncovalently linked molecular clusters of unique shape and composition and requires both a driving force and a dynamic system so that all possible molecular structures can be explored to generate the formation of the thermodynamically favored, ideally predesigned assembly.[1] An example of such a natural structure is the iron storage protein, apoferritin (Figure 1),[2] composed of 24 noncovalently linked protein subunits that form a nearly spherical shell of octahedral symmetry. We have described how a number of previously reported coordination clusters conform to the same principles that define the natural clusters and have shown how this can be used in de novo rational design of such clusters.[3,4] Here we summarize this approach, focusing on the most recent developments from our laboratory.

In the octahedral ferritin cluster, interaction of the protein subunits at the 4-fold axis can be considered a lock-and-key interaction in which the lock and key are 90° apart (Figure 1, left). The interaction around the 4-fold axis is both a symmetry and a stoichiometry requirement: it requires formation of tetramers from the monomeric subunit. Similarly, the interaction of the protein subunits at the 3-fold axis can be regarded as a lock-and-key interaction in which the lock and key are positioned 60° apart (Figure 1, right), requiring the formation of trimers. *Simultaneous satisfaction of these two incommensurate n-fold symmetry axes can only be achieved by formation of a cluster with octahedral symmetry.*

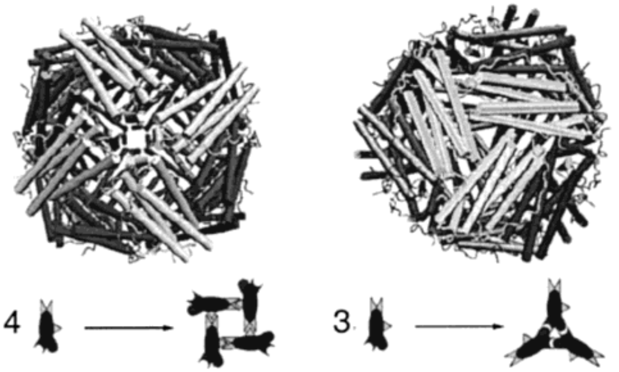

FIGURE 1. From the crystal structure of human H chain ferritin,[19] the octahedral 24-subunit iron storage protein as viewed down the 4-fold (left) and 3-fold (right) axes. The interaction at the 4-fold axis, in which the lock and key are 90° apart, requires the formation of tetramers. Similarly, the interaction at the 3-fold axis, in which the lock and key are 60° apart, requires the formation of trimers.

Rational Design of High-Symmetry Coordination Clusters

Protein−protein interactions are formed from many weak hydrogen bonds and van der Waals contacts along large regions or surfaces. However, the sum of these many individual interactions can be described by a single vectorial relationship, representing the geometry of the highly directional lock-and-key interactions described above. Metal−ligand interactions are strong and highly directional and can be used in place of many weak interactions to direct the formation of multimetal coordination clusters.

In principle, the formation of clusters of any symmetry should be possible. To do so, the symmetry elements of a particular point group need to be considered. To design a cluster with D_3 symmetry, an M_2L_3 triple helicate, for example, both the C_2 and C_3 axes of the point group must be taken into account. A C_2-symmetric bis(bidentate) ligand can provide the 2-fold axis, while a metal ion with pseudo-octahedral coordination by three bidentate chelators can provide the 3-fold axis. These symmetry axes *must*, however, be oriented 90° to one another. A cluster with T symmetry, an M_4L_6 tetrahedron, for example, is also possible with the same combination of symmetry elements. In this type of cluster, however, the C_2 and C_3 axes must be oriented 54.7° from one another.

Design Strategies

The metal coordination geometry and the orientation of the interaction sites in a given ligand provide the instructions, or blueprint, for the self-assembly of the proposed cluster. As a result, there are several important considerations in designing these supramolecular assemblies based

Dana L. Caulder was born in Columbia, South Carolina, in 1972. She earned a B.S. in chemistry from the University of South Carolina in 1994 and Ph.D. from the University of California, Berkeley, in 1998, where she was awarded a distinguished teaching award. Her Ph.D. thesis focused on the rational design of high-symmetry coordination clusters and the investigation of the unique kinetic and thermodynamic properties of these clusters. Currently she is a postdoctoral fellow at Lawrence Berkeley National Laboratory, where she is investigating the speciation and structure of actinide ions in proteins and wasteform glasses by synchotron radiation techniques.

Kenneth N. Raymond was born in 1942 in Astoria, Oregon. He obtained a B.A. from Reed College in 1964, and Ph.D. in 1968 from Northwestern University (with Basolo and Ibers). He was appointed Assistant Professor at the University of California, Berkeley, on July 1, 1967, becoming Associate Professor in 1974 and Professor in 1978. He has served as Vice Chair for the Berkeley Chemistry Department (1982−1984) and Chair (1993−1996). He was Chair of the ACS Division of Inorganic Chemistry in 1996. He received the Lawrence Award of the Department of Energy in 1984, a Humboldt Research Award in 1992, and the ACS Bader Award in Bioinorganic Chemistry in 1994 and was elected to the National Academy of Sciences in 1997. He has a long-standing interest in coordination chemistry, both synthetic and biological.

---

* To whom correspondence should be addressed. Phone: 510-642-7219. Fax: 510-486-5283. E-mail: raymond@socrates.berkeley.edu.

10.1021/ar970224v CCC: $18.00

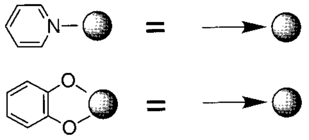

FIGURE 2. In the case of a monodentate ligand, the *coordinate vector* is the vector from the coordinating atom of the ligand directed toward the metal center. In the case of a bidentate ligand, the chelate vector is the vector that bisects the chelating group and is directed toward the metal ion.

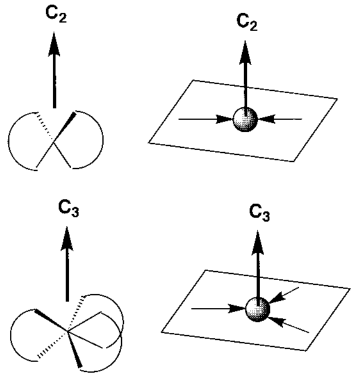

FIGURE 3. The plane orthogonal to the major symmetry axis of the metal complex is the *chelate plane*.

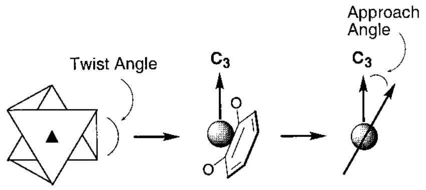

FIGURE 4. An alternative measure of the arrangement of three bidentate chelators around a metal ion is the *approach angle*.

on metal–ligand interactions. First, we choose to use multibranched *chelating* ligands because of their increased preorganization and stronger binding as a result of the chelate effect. Second, the orientation of the multiple binding units within a ligand must be rigidly fixed so that other, unwanted cluster stoichiometries or geometries are avoided. Third, because the self-assembly of the thermodynamically favored cluster involves the formation of many metal–ligand bonds, the metals should be labile so that mistakes resulting from the initial formation of kinetic products can be corrected. Catecholamide and hydroxamate ligands are excellent choices for binding units in supramolecular complexes because of the high stability and lability of these chelates with +3 metal ions with octahedral coordination environments.

As part of our approach, the feasibility of the proposed metal–ligand system is explored prior to ligand synthesis using molecular mechanics calculations.[5] Although these calculations do not guarantee that the proposed structure will form, they do help eliminate unsuitable targets. If the metal coordination and ligand geometry are correctly chosen, the intended supramolecular cluster should be the only structure that satisfies the binding requirements of the metal while not creating unfavorable steric interactions in the ligands.

Definitions

To describe this approach to rational design, it will be useful to define terms that precisely describe the relevant geometric relationships. The vector that represents the interaction between a ligand and metal is the *coordinate vector* (Figure 2). When using chelating ligands, the plane orthogonal to the major symmetry axis of a metal complex is the *chelate plane* (Figure 3); all of the coordinate vectors of the chelating ligands lie in the chelate plane. Any symmetric coordination complex cluster can be described in terms of the relationships between these chelate planes. In principle, by careful prearrangement of coordinate vectors in a multibranched ligand, programming of a cluster of any symmetry or stoichiometry becomes feasible.

Although the twist angle is a common measure of the arrangement of three bidentate chelators around a metal ion, the *approach angle* (Figure 4) has the advantage that it provides a measure that can be readily compared to angles generated by a given high-symmetry cluster. The approach angle is the angle between the vector connecting the two coordinating atoms of a bidentate ligand projected down the (pseudo) 2-fold axis of the chelate group and the major symmetry axis of the metal center. A twist angle of 60° corresponds to an approach angle of 35.3°, while a twist angle of 0° corresponds to an approach angle of 0°.

M_2L_3 Complexes

Triple Helicates. The simplest multimetal cluster contains two metal sites linked by one or more ligands. When these two metal ions are linked by three identical, C_2-symmetric ligand strands, the resulting bimetallic cluster is called a triple helicate if both metal ions have the same chirality. This chiral M_2L_3 complex has idealized D_3 symmetry: the C_3 axis is coincident with, and the three C_2 axes are perpendicular to, the helical axis of the complex.

To *rationally design* an M_2L_3 triple helicate with idealized D_3 symmetry, both C_2 and C_3 axes must be encoded into the ligand and metal components. Using a metal ion with pseudo-octahedral coordination and a C_2-symmetric bis(bidentate) ligand, these symmetry axes can be generated (vide supra). These symmetry axes *must*, however, be oriented 90° to one another. Because the two metal centers share the same C_3 helical axis, the two *chelate planes* in a triple helix must be parallel (Figure 5). Although a flexible linker may *allow* for the formation of an M_2L_3 triple helicate, a rigid linker can *direct* the formation of an M_2L_3 triple helicate.

Based on this design strategy, a series of M_2L_3 triple helicates based on ideally planar bis(bidentate) catecholamide ligands has been synthesized (H_4**1**–H_4**7**, Figure 6).[6–8] The rigid aromatic linkers serve to maintain preorganization of the ligand, since other topologies are possible when flexible linkers are used. The chelate vectors, indicated as arrows, are parallel and point in the same direction within each ligand. Molecular mechanics

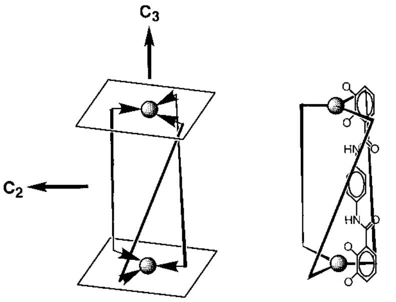

FIGURE 5. In a D_3-symmetric triple helicate, the chelate planes are parallel. The spheres represent the pseudo-octahedral metal ions, the rods represent the ligands, and the arrows on the ligand rods indicate the coordinate vectors.

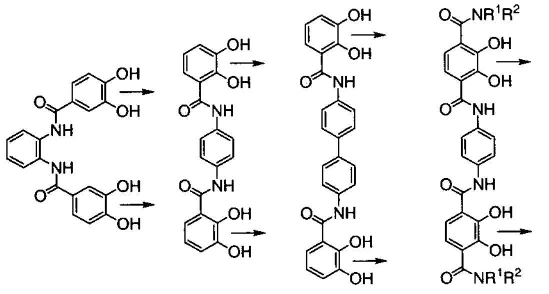

$H_4$1 **$H_4$2** **$H_4$3** **$H_4$4** $R^1=R^2=H$
$H_4$5 $R^1=R^2=Pr^i$
$H_4$6 $R^1=Pr^i$, $R^2=Me$
$H_4$7 $R^1=R^2=(S)\text{-}CHMePh$

FIGURE 6. Rigid bis(catecholamide) ligands designed to form M_2L_3 triple helicates. The fixed distance between the catechol groups is sufficient information to generate an ordered system.

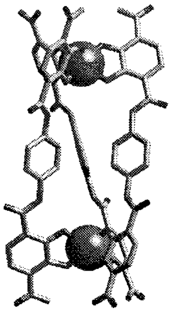

$[Ga_2\mathbf{4}_3]^{6-}$

FIGURE 7. Crystal structure of the triple helicate $[Ga_2\mathbf{4}_3]^{6-}$.

calculations indicated that, for each of these ligands, the chiral helicate was lower in energy than the meso-M_2L_3 cluster.[5] The M_2L_3 stoichiometry was confirmed by both fast atom bombardment and electrospray mass spectrometry. The crystal structure[6,7] of the Ga(III) complex of $H_4\mathbf{4}$ is shown in Figure 7 and confirms that the rigid ligand forms a racemic mixture of homochiral triple helicates with Ga(III).

Triple Mesocates. A *nonchiral* M_2L_3 cluster has a Δ-configuration at one metal center and a Λ-configuration at the other and, therefore, will be called a *meso*-complex or a mesocate. This type of cluster has idealized C_{3h} symmetry: Rather than having three C_2 axes perpendicular to the C_3 axis, there is an orthogonal mirror plane that relates the Δ- to the Λ-configured metal center.

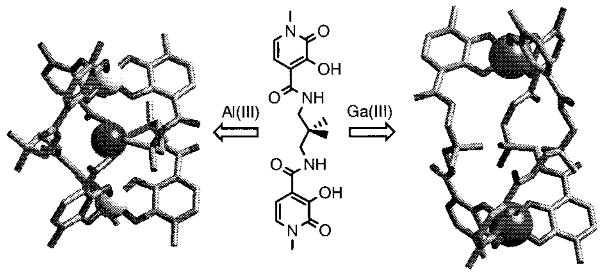

$H_2O \subset (\Delta\Delta,\Lambda\Lambda)\text{-}Al_2\mathbf{8}_3$ $H_2\mathbf{8}$ $(\Delta\Lambda)\text{-}Ga_2\mathbf{8}_3$

FIGURE 8. Ligand $H_2\mathbf{8}$ forms both a chiral helicate (left) and an achiral mesocate (right).[9] The pictures are based on the X-ray structure coordinates. The $Al_2\mathbf{8}_3$ helicate has a molecule of water in the cluster cavity, similar to a previously reported iron(III) complex of a rhodotorulic acid analogue.[20]

Recently we have presented the first example of a ligand ($H_2\mathbf{8}$) that makes *both* a helicate and a mesocate.[9] Remarkably, the X-ray analysis showed that, in the solid state, the $Al_2\mathbf{8}_3$ complex is a chiral helicate (racemic), while the $Ga_2\mathbf{8}_3$ complex is an achiral mesocate (Figure 8). Although both complexes contain the same ligand, the structures are markedly different: the distance between the two metal centers in $Al_2\mathbf{8}_3$ is 7.13 Å, while in $Ga_2\mathbf{8}_3$ this distance is 9.74 Å. The structures show that the helical cavity of $Al_2\mathbf{8}_3$ contains one encapsulated water molecule, while no encapsulated solvent was found in the $Ga_2\mathbf{8}_3$ mesocate (Figure 8).

M_4L_6 Complexes

Another cluster with the same metal-to-ligand ratio as the M_2L_3 triple helicate is the M_4L_6 tetrahedron, where the four metal ions act as the vertices and the six ligands act as the edges of a tetrahedron. Depending on the chiralities at the metal centers, the cluster can have either idealized C_3 (ΔΛΛΛ/ΛΔΔΔ), S_4 (ΔΔΛΛ), or T (ΛΛΛΛ/ΔΔΔΔ) symmetry.

We have demonstrated the utility of our model in two approaches to the *rational design* of such clusters. Both approaches employ an ideally planar C_2-symmetric bis(bidentate) ligand with a rigid backbone, but the orientation of the C_2 axis of the cluster with respect to the plane of the ligand differs. In the first design strategy, the 2-fold axis of the tetrahedron is intended to be coplanar with the plane defined by the ligand (Figure 9). Since the chelate vectors must lie within the chelate planes at each of the four metal vertices, the angle between the chelate vectors within a given ligand must be 70.6°. A 60° angle is formed for ligand $H_2\mathbf{9}$ (Figure 10); thus, the targeted structure can be achieved with only slight out-of-plane twisting by each of the chelating groups.

The crystal structure of $Ga_4\mathbf{9}_6$ revealed that the tetrahedral cluster has S_4 symmetry (two Δ and two Λ metal centers) in the solid state (Figure 11). The ligand backbone is coplanar with the S_4 axis, and there is a substantial cavity, which is partially open to the outside, in the cluster. Four crystallographically identical DMF molecules partially fill the cavity.

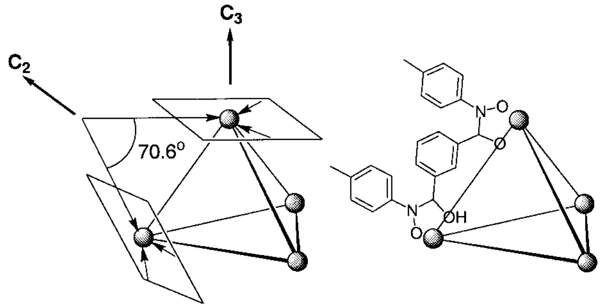

FIGURE 9. One approach to the synthesis of M_4L_6 tetrahedral clusters relies on the plane of the ligand being coincident with the 2-fold axis of the tetrahedral cluster. As such, the coordinate vectors within a given ligand must be oriented 70.6° from each other.

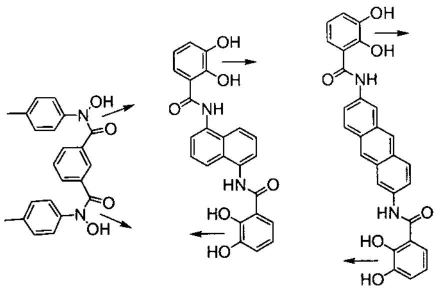

H_2**9** H_4**10** H_4**11**

FIGURE 10. Ligands designed to form M_4L_6 tetrahedral clusters. In each case, the ligand has C_2 symmetry. How that symmetry conforms to the cluster geometry determines the properties of the cluster.

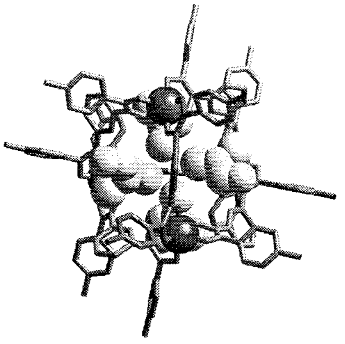

4DMF ⊂ Ga_4**9**$_6$

FIGURE 11. Viewed down the crystallographic S_4 axis, the structure of Ga_4**9**$_6$ shows four DMF solvent molecules pointing into the cluster cavity.[15]

In the second design strategy, the 2-fold axis of the tetrahedron is designed to be perpendicular to the ligand plane. The ideally planar ligand should have antiparallel coordinate vectors. To understand this design, it helps to view the tetrahedral cluster as a truncated polyhedron (Figure 12). If the six ligands are to act as the six 2-fold symmetric faces of the polyhedron, then the angle between the chelate planes is no longer important. The angle between the extended 2-fold plane and the C_3 axis of the cluster *is* important, however, as this corresponds to the approach angle. This approach angle is 35.3° and corresponds to a perfect octahedral metal complex with a 60° twist angle. Clusters based on this design should be homochiral with idealized *T* symmetry (i.e., all Δ or all Λ metal centers).

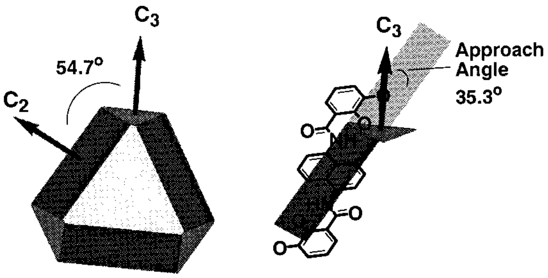

FIGURE 12. An M_4L_6 cluster can be envisioned in which the six ligands act as the six 2-fold symmetric faces of the truncated polyhedron.

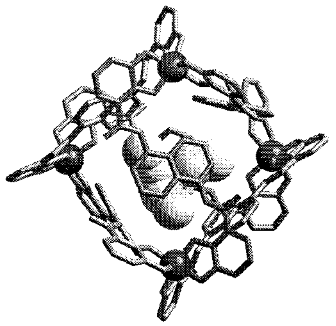

$Et_4N^+ \subset [Fe_4$**10**$_6]^{12-}$

FIGURE 13. H_4**10** forms an M_4L_6 tetrahedral cluster with Ga(III) and Fe(III). The crystal structure of the $[Fe_4$**10**$_6]^{12-}$ cluster with the encapsulated Et_4N^+ is shown.

Ligands H_4**10**[10] and H_4**11**[11] (Figure 10) were designed to form M_4L_6 tetrahedral clusters based on this strategy. Solution- and solid-state observations showed that one of the Et_4N^+ counterions is encapsulated within the $[M_4$**10**$_6]^{12-}$ (M = Ga(III), Fe(III)) cluster interior. In the crystal structure of $K_5(Et_4N)_7[Fe_4$**10**$_6]$ (Figure 13), the naphthalene rings of the ligands are twisted around the arene–N bond so that they are in van der Waals contact with the encapsulated Et_4N^+. The distance between the iron atoms in the *T* symmetry cluster is 12.8 Å.

In an attempt to make a similar cluster with a larger cavity, ligand H_4**11** (Figure 10), based on a 2,7-diaminoanthracene backbone, was prepared. This ligand also forms an M_4L_6 tetrahedral cluster, but *only* in the presence of an alkylammonium guest! In the crystal structure of $K_4(Me_4N)_8[Ti_4$**11**$_6]$ (Figure 14), one molecule of Me_4N^+ is located in the cavity of the *T* symmetry cluster. The distance between the titanium atoms averages 16.1 Å. However, in the absence of an alkylammonium guest molecule, H_4**11** forms an M_2L_3 triple helicate with Ti(IV) (Figure 14).[11] Although the metal centers within a given complex have the same chirality, the overall structure is significantly distorted from idealized D_3 geometry. It is apparent that the greater bridge length and flexibility of the anthracene ligand allow for the formation of the M_2L_3 structure, but just barely.

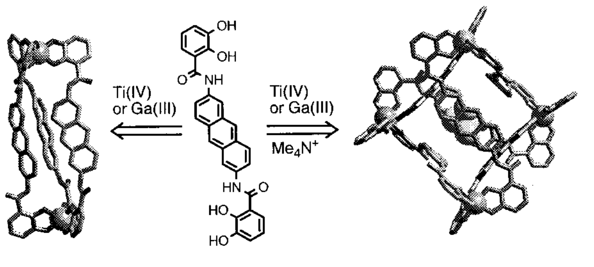

$[Ti_2\mathbf{11}_3]^{4-}$ $H_4\mathbf{11}$ $Me_4N^+ \subset [Ti_4\mathbf{11}_6]^{8-}$

FIGURE 14. Ligand $H_4\mathbf{11}$ forms an M_2L_3 helicate in the absence of Me_4N^+ guest but an M_4L_6 tetrahedron in the presence of Me_4N^+. The crystal structures of $[Ti_2\mathbf{11}_3]^{4-}$ (left) and $Me_4N^+ \subset [Ti_4\mathbf{11}_6]^{8-}$ (right) are shown.[11]

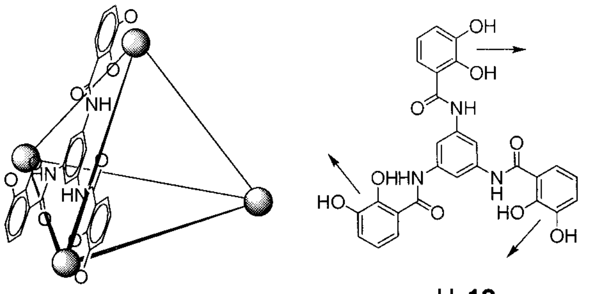

$H_6\mathbf{12}$

FIGURE 15. An M_4L_4 tetrahedral cluster with the metals on the vertices and ligands on the faces of the tetrahedron is formed from ligand $H_6\mathbf{12}$.

M_4L_4 Complexes

An approach to the synthesis of M_4L_4 tetrahedral clusters has also been developed. In an M_4L_4 tetrahedral cluster, the metal ions occupy the four vertices, and the ligands occupy each of the four faces of the tetrahedron (Figure 15), implying that both the ligand and the metal ion must have 3-fold symmetry. As in the previously described M_2L_3 helicates and M_4L_6 tetrahedra, three bidentate ligands coordinating a pseudo-octahedral metal ion can generate a 3-fold axis at the metal. Rather than using a C_2-symmetric ligand, a C_3-symmetric ligand can be utilized. This ligand must be rigid, however, so that no two chelating moieties on the ligand can coordinate a single metal ion. Ligand $H_6\mathbf{12}$ satisfies this requirement (Figure 15).[12] If the ligand is ideally planar, as in the case of $H_6\mathbf{12}$, then the approach angle for this type of cluster is 19.4° (Figure 16, left). This ideal angle is less than 4° from the approach angle of 23° (corresponding twist angle = 40°) observed for tris(catecholate) complexes of Ti(IV), Ga(III), and Fe(III); therefore, this design seems optimized for metal ions with significant distortions toward trigonal prismatic geometry.

The Al(III), Fe(III), Ga(III), Ti(IV), and Sn(IV) complexes of $H_6\mathbf{12}$ were prepared, and X-ray quality crystals were obtained of the $(Et_3NH)_8[Ti_4\mathbf{12}_4]$ complex (Figure 16, right).[12] The cluster is a racemic mixture of homochiral tetrahedra (either all Δ or all Λ configuration within a given cluster). There is no evidence that the small cavity of the tetrahedron contains a guest.

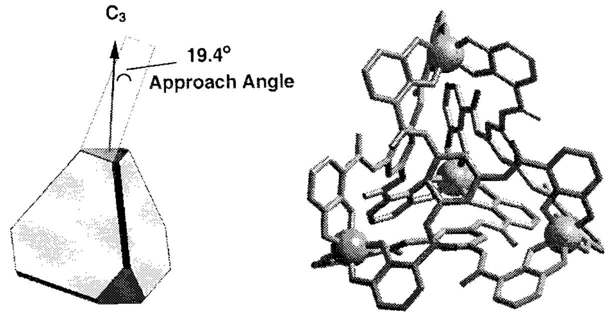

$[Ti_4\mathbf{12}_4]^{8-}$

FIGURE 16. If the ligand is ideally planar, as in the case of $H_6\mathbf{12}$, then the angle that the 3-fold face of the tetrahedron makes with the C_3 axis is 19.4° and corresponds to the approach angle. The crystal structure of $[Ti_4\mathbf{12}_4]^{8-}$ is shown (right).[12]

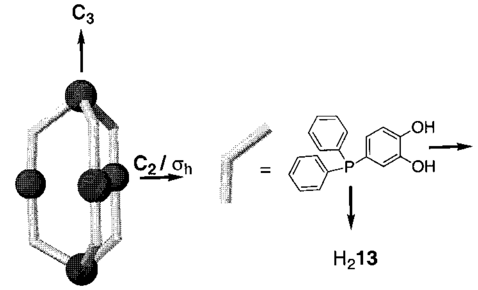

$H_2\mathbf{13}$

FIGURE 17. A cluster with D_3 (or C_{3h}) symmetry can be designed using an asymmetric ligand $H_2\mathbf{13}$.[13] Interaction of the catechol moiety with an octahedral metal ion can generate the necessary C_3 axis, while interaction of the phosphine moiety with a square planar metal ion can generate the C_2 axis (or mirror plane). Simultaneous satisfaction of these two symmetry requirements can lead to a cluster with D_3 (or C_{3h}) symmetry.

Two-Metal Clusters

We have recently demonstrated the rational design of an $M_2M'_3L_6$ mixed-metal cluster in which, rather than using a symmetric *ligand* to generate a symmetry element, two *different metals* generate the two symmetry elements (Figure 17).[13] In principle, the ligand $H_2\mathbf{13}$ forms part of an asymmetric unit of the cluster and must have two different symmetry interaction sites. As described earlier, a chiral triple helicate has idealized D_3 symmetry, while an achiral triple mesocate has C_{3h} symmetry. Therefore, to synthesize a mixed-metal helicate (or mesocate) of stoichiometry $M_2M'_3L_6$, one must consider a 3-fold interaction site and an orthogonal 2-fold (or mirror plane) interaction site (Figure 17).

Catechol ligands are relatively hard donors and generate a C_3 axis when forming a tris-chelate with hard, trivalent, or tetravalent metals (e.g., Al(III), Ga(III), Fe(III), Sn(IV), Ti(IV)). Phosphine ligands, on the other hand, are soft donors and can generate a 2-fold axis or mirror plane when coordinated to a square planar metal (e.g., Pd(II) or Pt(II)) in a trans fashion. A ligand containing both of these functionalities arranged in the proper geometry can assemble an $M_2M'_3L_6$ cluster, because it is the smallest discrete species that would simultaneously fulfill the two orthogonal symmetry requirements.

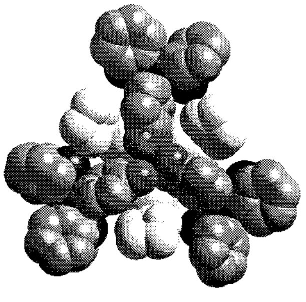

$3(Cs{\bullet}2THF) \subset [Ti_2\mathbf{13}_6(PdBr_2)_3]^{4-}$

FIGURE 18. Viewed down the crystallographic 3-fold axis, this space-filling model shows the buried cesium cations and their coordinated THF molecules (lightly shaded).[13]

The crystal structure of $Cs_4[Ti_2\mathbf{13}_6(PdBr_2)_3]$ shows that the complex has C_{3h} symmetry; the cluster is a mesocate with one of the titanium atoms having Δ and the other having Λ configuration. Interestingly, three of the Cs^+ counterions are located in clefts of the cluster (Figure 18). Each is coordinated by four of the catecholate oxygens and two molecules of THF. The clefts of the cluster are so deep that the coordinating THF molecules can also be described as being buried. The palladium-coordinated bromine atoms are not in van der Waals contact with the cesium atoms, but they do shield the cesium atoms from other potentially coordinating solvent molecules, helping to explain the low coordination number (6) of the Cs^+ cations.

Dynamics of Supramolecular Clusters

The geometric requirements for synthesizing clusters of various stoichiometries and symmetries are beginning to be understood. It is less clear, however, how these clusters assemble in solution from the ligand and metal components and, once assembled, how the clusters function. For example, how is geometric information transmitted between the multiple coordination sites of a given ligand? Is there coupling of the isomerization of chiral metal centers, and, if so, what is the magnitude of this coupling as transmitted through the rigid ligand? For clusters that recognize and encapsulate guest molecules, what are the factors controlling the recognition process, and how do guests enter and exit the cluster cavity?

M_2L_3 Triple Helicate Stereoisomerism Dynamics. When using rigid ligands to synthesize triple helicates, the chirality of the first metal center should induce the same chirality at the second metal center, so that only $\Delta\Delta$- and $\Lambda\Lambda$-configured complexes are present. The magnitude of the mechanical coupling between the two metal centers and the mechanism of the inversion reaction have been investigated using the dinuclear Ga(III) complexes of ligands $H_4\mathbf{5}-H_4\mathbf{7}$ and similar mononuclear Ga(III) complexes based on simple bidentate catecholamide ligands.[6,7,14] The methyl groups on the isopropyl substituents of $H_4\mathbf{5}$ are rendered diastereotopic around the chiral metal center.

The activation parameters for this process are not solvent dependent, consistent with an intramolecular mechanism. The free energy inversion barrier ($\Delta\Delta \leftrightarrow \Lambda\Lambda$) for $K_6[Ga_2\mathbf{5}_3]$ in DMSO-d_6 (79.8 kJ mol^{-1}) or D_2O solutions (78.7 kJ mol^{-1}, $pD = 12.1$) is only 1.2 times higher compared to that for the corresponding mononuclear complex. The kinetic data show weak coupling of both metal centers that is about 22.6 kJ mol^{-1}. Thus, it is concluded that inversion of the Λ,Λ- and Δ,Δ-$[Ga_2\mathbf{5}_3]^{6-}$ helicates involves the heterochiral Λ,Δ-$[Ga_2\mathbf{5}_3]^{6-}$ anion as an intermediate, which is produced by a single twist event along the reaction pathway.

At lower pD, a second mechanism becomes dominant in D_2O. In contrast to the mononuclear complex, the dinuclear $K_6[Ga_2\mathbf{5}_3]$ helicate shows a second-order proton dependence below $pD = 7$. Inversion of one center, which occurs rapidly because of the single protonation, does not change the overall chirality, owing to the higher energy of the heterochiral intermediate and its consequent short lifetime. Only when the second metal center is also protonated can the overall inversion of the helicate occur. In the absence of mechanical coupling of the metal centers, only a single proton dependence would be expected because the heterochiral intermediate would have the same energy as the homochiral anions and, consequently, a long lifetime.

***rac*-($\Delta\Delta/\Lambda\Lambda$)-$M_2L_3$ Helicate to $\Lambda\Delta$-M_2L_3 Mesocate Interconversion Dynamics.** As noted earlier, in the solid state $H_2\mathbf{8}$ forms a helicate with Al(III) but a mesocate with Ga(III) (Figure 8).[9] The methyl substitutents in the $H_2\mathbf{8}$ backbone serve as markers for following the solution structure of the metal complexes by ^1H NMR; in the helicate these two methyl groups are equivalent, while in the mesocate the methyl groups are diastereotopic. As expected for the mesocate, the ^1H NMR spectrum of $Ga_2\mathbf{8}_3$ in DMSO-d_6 shows two singlets for the methyl groups in the ligand spacer; however, the presence of an additional singlet indicates that the helicate form of this complex is also present in solution. Variable-temperature ^1H NMR experiments reveal that these two structures are in thermodynamic equilibrium, with the helicate being preferred at high temperatures. Additional investigations revealed that the spontaneous *meso*-to-helix conversion is an entropy-driven process, which must be a consequence of different numbers of solvent molecules associated with the two forms of the complex.[9] Crystal structures of a helicate ($H_2O{\subset}Al_2\mathbf{8}_3$) and mesocate ($Ga_2\mathbf{8}_3$) complex of $H_2\mathbf{8}$ support this conclusion: the helicate exterior appears more hydrophobic than the mesocate and consequently would have fewer polar water molecules associated with it in solution compared to the mesocate.

Stereoisomerism in M_4L_6 Tetrahedral Clusters. As described, the M_4L_6 tetrahedral cluster based on ligand $H_2\mathbf{9}$ crystallizes as the S_4 isomer ($\Delta\Delta\Lambda\Lambda$ chiralities at the four metal vertices).[15] Low-temperature ^1H NMR experiments reveal, however, that $Ga_4\mathbf{9}_6$ is a mixture of T ($\Delta\Delta\Delta\Delta/\Lambda\Lambda\Lambda\Lambda$), C_3 ($\Delta\Lambda\Lambda\Lambda/\Lambda\Delta\Delta\Delta$), and S_4 ($\Delta\Delta\Lambda\Lambda$) isomers in solution ($CDCl_3$).[16] With decreasing temperature, the broad resonance of one of the ligand protons, which is pointing into the cavity, splits into five distinct peaks, representing the three isomers. Although the isomers are not present in *exact* statistical distribution, the distribution shows that the stability of the three isomers is very similar, and, therefore, the mechanical coupling between the metal centers is negligible.

Ligand exchange in hydroxamate iron(III) complexes has been previously studied,[17] but isomerization of a simple tris-hydroxamate iron(III) or gallium(III) complex is certainly too fast to follow by NMR. The slower rate of interconversion detected here can be attributed to the geometric properties of the ligand and the cluster. In order for a metal center to change its chirality, it must pass through a trigonal prismatic transition state. Since four coordination centers are tethered in the tetrahedron, the Bailar twist is the only mechanically possible rearrangement. To do this, the ligands in contact with the active metal *must* pass through a conformation in which the ligand's two chelate vectors cannot coexist in the chelate planes of each metal center. In effect, because the ligand maintains an angle of only 60° in its planar form, it forces a very distorted trigonal prismatic intermediate.

To isomerize from ΔΔΔΔ to ΛΛΛΛ, the cluster has to go through all intermediate stereoisomers. NMR observations and MM2 calculations suggest that all of these isomers are very close in energy. We can also assume (and results confirm) that isomerization of ΔΔΛΛ to ΔΔΔΛ will have the same energy barrier as its isomerization to ΔΛΛΛ, since both processes require inversion of configuration at only one metal center. Further, the inversion from ΔΔΔΛ to ΔΔΔΔ must have the same energy barrier as inversion of ΔΛΛΛ to ΛΛΛΛ, since these are mirror image processes. Coalescence of the ^{1}H NMR resonances is observed at 300 K, corresponding to an activation barrier of 58 kJ mol^{-1} for the inversion processes at each metal vertex.

Self-Recognition in M_2L_3 Triple Helicates. A different issue of designed order was addressed in a family of helicate complexes of varying, but fixed, metal−metal distances. It was intended that the information stored in rigid bis(catecholamide) ligands (H_4**1**−H_4**3**, Figure 6) be used to overcome the intrinsic disorder of mixtures to produce a highly ordered system of complexes in solution.[8] These ligands are unique in that, because of the rigidity and varying distances between the catecholamide functionalities, it is geometrically impossible to form a mixed ligand $(M_2L_2L'_1)^{6-}$ complex. When mixtures of any two or all three of the ligands shown in Figure 6 are equilibrated at room temperature with $Ga(acac)_3$ in basic methanol, both ^{1}H NMR spectroscopy and electrospray mass spectrometry indicate that only the individual complexes form (Figure 19). Remarkably, no oligomeric or mixed-ligand species are observed in solution.

Selective Encapsulation of Alkylammonium Guests by a Tetrahedral Cluster Host. The tetrahedral cluster $[Ga_4\mathbf{10}_6]^{12-}$ shows remarkable discrimination between alkylammonium guests.[10] There are orders of magnitude differences between the association equilibrium constants, K_{eq}, for Me_4N^+, Et_4N^+, and Pr_4N^+, and these differences allow for the quantitative stepwise exchange of one guest for another (Figure 20). If Pr_4N^+ is added to a solution of $K_6(Me_4N)_6[Ga_4\mathbf{10}_6]$, the Pr_4N^+ quickly (<1 min) and quantitatively is incorporated into the cluster cavity, displacing Me_4N^+. In turn, if Et_4N^+ is added to this same solution, the Et_4N^+ displaces the Pr_4N^+ rapidly (<1 min) and quantitatively! In the presence of either Me_4N^+, Et_4N^+, or Pr_4N^+, the tetrahedral cluster selectively encapsulates Et_4N^+. No mixtures are observed by ^{1}H NMR.

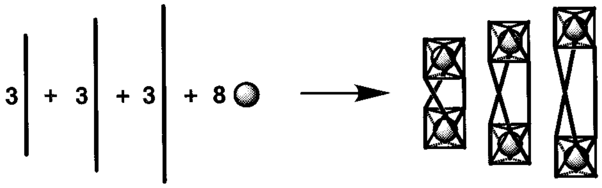

FIGURE 19. Schematic representation of self-recognition in gallium(III) triple helicates. The different sized rods represent the different length ligands. Spheres represent the gallium ions.

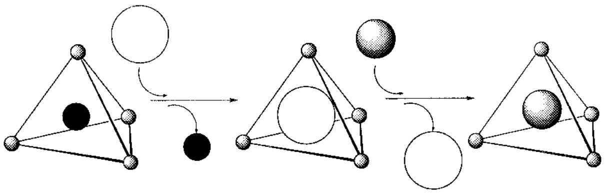

FIGURE 20. Schematic representation of stepwise guest exchange from the cavity of the tetrahedral cluster $[Ga_4\mathbf{10}_6]^{12-}$ The small black spheres represent Me_4N^+, the large white spheres Pr_4N^+, and the intermediate shaded spheres Et_4N^+.

The thermodynamic parameters for the inclusion reaction in water have been determined by measuring the temperature dependence of the association equilibrium constants (K_{eq}).[18] In the absence of any other guests, the cavity of the $[Ga_4\mathbf{10}_6]^{12-}$ host will most likely be filled with solvent molecules. The van't Hoff plots for the encapsulation of $Me_2Pr_2N^+$, Pr_4N^+, and *N,N,N′,N′*,-tetramethyl-1,3-propanediammonium by the host $[Ga_4\mathbf{10}_6]^{12-}$ anion show that encapsulation of the cationic guests into this dodecaanion is an *endothermic* process. The enthalpies and entropies are both positive; the encapsulation is an entropy-driven process. How is it that the encapsulation of cations by a host with a −12 charge can be endothermic? The answer lies in the very large and dominant solvation enthalpies of the ions. The free energy of hydration predicted by the Born equation is $-162z^2r^{-1}$ kcal mol^{-1}, where z are units of charge and r is the diameter of the ion in angstroms. The corresponding entropy of hydration is $-2.8z^2r^{-1}$ kcal mol^{-1} at 298 K, predicting a ΔH of hydration of $-165z^2r^{-1}$ at 298 K. Because ΔH of hydration is z^2 dependent, solvation of the −12 anion is the largest term. This term and the cation solvation energy override the enthalpy gained on partial charge neutralization. This model also makes a clear prediction that higher charge cations will not be encapsulated and that highly solvated, singly charged cations (e.g., K^+) should be poor guests.

Guest-Induced M_2L_3 Helicate-to-M_4L_6 Tetrahedron Conversion. We have shown that two different clusters, a triple helicate and a tetrahedron, can be prepared using identical ligand (H_4**11**) and metal components (Figure 14).[11] Simply the addition of an appropriate guest is enough to shift the equilibrium from the entropically preferred helicate to the tetrahedron! The gallium(III) analogues were prepared because of the greater lability of Ga(III) compared to Ti(IV). The addition of 20 equiv of Me_4NCl to a $K_6[Ga_2\mathbf{11}_3]$ solution in D_2O revealed that complete transformation of the helicate into the tetrahedral cluster occurred after 5 days.

Summary

In this Account, we have illustrated the utility and generality of an approach to the *designed* synthesis of supramolecular clusters based on metal−ligand interactions. An analysis of the high symmetry seen in the natural protein clusters, such as ferritin, is based on the incommensurate symmetry numbers of the interaction sites and the fixed relative angles between these symmetry axes. The use of this model in the successful design of several metal−ligand clusters has been illustrated. Rigid ligand geometries, while chosen to accommodate the targeted cluster geometry, preclude the formation of alternative structures. This process is greatly facilitated by molecular modeling in the early stages of design.

The initial investigation of the dynamic behavior of these synthetic supramolecular clusters lets us begin to understand the mechanical coupling between chiral metal centers in M_2L_3 and M_4L_6 clusters, the kinetics and host−guest chemistry of multimetal complexes, the self-recognition properties in predesigned rigid systems, and the dramatic role that guest molecules can play in the formation of clusters of $n(M_xL_y)$ ($n = 1, 2, 3, ...$) stoichiometries.

The host−guest chemistry of these clusters offers the first promise of achieving synthetically what is accomplished by natural supramolecular clusters. The natural clusters protect valuable guest molecules by providing a nanometer-scale environment that is significantly different from the surrounding solution. We have seen the first indications that the properties of the guest molecules can be altered in our synthetic host clusters. The further development of the reaction chemistry of the encapsulated guests is an exciting prospect.

This research is supported by the National Science Foundation through Grant No. CHE-9709621 and the exchange grants from NATO (SRG 951516) and NSF (INT-9603212). We acknowledge the contributions of our co-workers, who are cited in the referenced publications discussed in this Account.

References

(1) Lehn, J.-M. *Supramolecular Chemistry: Concepts and Perspectives*; VCH: Weinheim, 1995.
(2) Proulxcurry, P. M.; Chasteen, N. D. Molecular Aspects and Iron Uptake and Storage in Ferritin. *Coord. Chem. Rev.* **1995**, *144*, 347.
(3) Caulder, D. L.; Raymond, K. N. The Rational Design of High Symmetry Coordination Clusters. *J. Chem. Soc., Dalton Trans.* **1999**, 1185−1200. Many of the figures, originally in color, and some of the text of this brief presentation originate from this full review.
(4) Raymond, K. N.; Caulder, D. L.; Powers, R. E.; Beissel, T.; Meyer, M.; Kersting, B. Coordination Number Incommensurate Cluster Formation. *Proc. 40th Robert A. Welch Found. Chem. Res.* **1996**, *40*, 115−129.
(5) *CAChe 4.0*; Oxford Molecular Group, Inc.: Campbell, CA, 1997.
(6) Kersting, B.; Meyer, M.; Powers, R. E.; Raymond, K. N. Dinuclear Catecholate Helicates: Their Inversion Mechanism. *J. Am. Chem. Soc.* **1996**, *118*, 7221.
(7) Meyer, M.; Kersting, B.; Powers, R. E.; Raymond, K. N. Rearrangement Reactions in Dinuclear Triple Helicates. *Inorg. Chem.* **1997**, *36*, 5179−5191.
(8) Caulder, D. L.; Raymond, K. N. Supramolecular Self-Recognition and Self-Assembly in Gallium(III) Catecholamide Triple Helices. *Angew. Chem., Int. Ed. Engl.* **1997**, *36*, 1439−1442.
(9) Xu, J.; Parac, T.; Raymond, K. N. *Angew. Chem., Int. Ed. Engl.*, submitted for publication.
(10) Caulder, D. L.; Powers, R. E.; Parac, T. N.; Raymond, K. N. The Self-Assembly of a Pre-designed Tetrahedral M_4L_6 Supramolecular Cluster. *Angew. Chem., Int. Ed. Engl.* **1998**, *37*, 1840−1843.
(11) Scherer, M.; Caulder, D. L.; Johnson, D. W.; Raymond, K. N. Triple Helicate−Tetrahedral Cluster Interconversion Controlled by Host−Guest Interactions. *Angew. Chem., Int. Ed. Engl.* **1999**, *38*, 1587−1592.
(12) Brückner, C.; Powers, R. E.; Raymond, K. N. The Designed Formation of a Tetrahedral Ti_4L_4 Cluster. *Angew. Chem., Int. Ed. Engl.* **1998**, *37*, 1837−1839.
(13) Sun, X.; Johnson, D. W.; Caulder, D. L.; Powers, R. E.; Raymond, K. N.; Wong, E. H. Exploiting Incommensurate Symmetry Numbers: Rational Design and Assembly of $M_2M'_3L_6$ Supramolecular Clusters with C_{3h} Symmetry. *Angew. Chem., Int. Ed. Engl.* **1999**, *38*, 1303−1307.
(14) Kersting, B.; Telford, J. R.; Meyer, M.; Raymond, K. N. Gallium(III) Catecholate Complexes as Probes for the Kinetics and Mechanism of Inversion and Isomerization of Siderophore Complexes. *J. Am. Chem. Soc.* **1996**, *118*, 5712−5713.
(15) Beissel, T.; Powers, R. E.; Raymond, K. N. Symmetry-Based Metal Complex Cluster Formation. *Angew. Chem., Int. Ed. Engl.* **1996**, *35*, 1084−1086.
(16) Beissel, T.; Powers, R. E.; Parac, T. N.; Raymond, K. N. Dynamic Isomerization of a Supramolecular Tetrahedral M_4L_4 Cluster. *J. Am. Chem. Soc.* **1999**, *121*, 4200−4206.
(17) Caudle, M. T.; Crumbliss, A. L. Dissociation Kinetics of (*N*-Methylacetohydroxamato)iron(III) Complexes. *Inorg. Chem.* **1994**, *33*, 4077−4085.
(18) Parac, T. N.; Caulder, D. L.; Raymond, K. N. Selective Encapsulation of Aqueous Cationic Guests into a Supramolecular Cluster. *J. Am. Chem. Soc.* **1998**, *120*, 8003−8004.
(19) Lawson, D. M.; Artymiuk, P. J.; Yewdall, S. J.; Smith, J. M. A.; Livingstone, J. C.; Treffry, A.; Luzzago, A.; Levi, S.; Arosio, P.; Cesarini, G.; Thomas, C. D.; Shaw, W. V.; Harrison, P. M. Solving the Structure of Human H Ferritin by Genetically Engineering Intermolecular Crystal Contacts. *Nature* **1991**, *349*, 541−544.
(20) Scarrow, R. C.; White, D. L.; Raymond, K. N. Ferric Ion Sequestering Agents. 14. 1,2-HOPO Complexes: Properties and Structure of a Novel FeFe Dimer. *J. Am. Chem. Soc.* **1985**, *107*, 6540−6546.

AR970224V